Gain Enhancement of Patch Antenna using Novel Glass Fiber Reinforced Polymer (GFRP) based Metasurface

Abul Khair Muhammad Shafaat Ali[1], Irfan Ahmed[2], Sundus Ali[3], Mobin Khalid[3]
[1]Department of Electronic Engineering, NED University of Engineering and Technology, Karachi, Pakistan
[2]Department of Physics, NED University of Engineering and Technology, Karachi, Pakistan
[3]Department of Telecommunications Engineering, NED University of Engineering and Technology, Karachi, Pakistan

Corresponding author: Sundus Ali (e-mail: sundus@neduet.edu.pk).

ABSTRACT In this paper, the authors have presented extensive work done involving the design, simulation, development, and gain performance measurement of a novel Glass Fiber Reinforced Polymer (GFRP) composite based metasurface patch antenna. The authors have first designed GFRP composite based metasurface patch antenna and simulated the design to measure its gain performance and then the same antenna has been manufactured by following the design specifications. We have designed, optimized, manufactured and tested C-band rectangular patch antenna using COTS substrate first. Later, GFRP based composite was used as metasurface on top of the rectangular patch antenna and the design was optimized and a measurement for gain performance enhancement in terms of antenna gain was analyzed. Finally, another layer of GFRP composite sample was added up on the top of metasurface patch antenna and measurement results for antenna gain improvement was discussed and comparison was done. The results obtained through simulation and testing show characteristic similarity thus validating the approach adopted for the printing of copper on GFRP composite. The results also show that using GFRP composite as a metasurface on top of simple microstrip patch antenna results in an overall 39% gain enhancement compared to simple microstrip patch antenna gain.

INDEX TERMS Design, Development, Gain, GFRP, Metasurface, Patch antenna.

I. INTRODUCTION

MODERN day communication systems are becoming more compact, lightweight and robust [1], [2]. In addition to this, an increase in demand for systems to deliver high data rate [3], support ultra-wideband communication [4], and frequency configurability features [5] makes it much more challenging for the RF design engineers to come up with such solutions which not only meet these technical requirements but also satisfy modern day aesthetics To meet these requirements for future communication systems, technological advancements have been made, among which lightweight materials [6] availability is most promising as it makes it possible to design lightweight and reliable communication systems.

Nowadays, there are many technical solutions applied in the antenna construction to satisfy the requirements of modern communication systems, as they are considered an important and critical component of wireless communication systems. One of the performance indicators is improving the gain of antenna, which has been the goal of many researchers in recent years. Conventional single element microstrip antenna without the addition of any loads between the patch and ground plane provides a conventional fixed gain at a designed narrow frequency band. With the introduction of loads (pins, varactor diodes and adaptive elements) in the microstrip antenna, results in variable resonant frequency [7], impedance [8], polarization and pattern. To achieve any of these performance improvements in microstrip antenna, biasing is required of these loads.

More recently, metasurface antennas [9], [10], [11] are used to achieve enhancement in different antenna performance parameters including gain improvement [12], bandwidth improvement [12], better aperture efficiency [13] and frequency reconfiguration [14]. Metasurface antennas are 2D planar structures and are usually used in microstrip antenna applications.

Generally, Commercial of the Shelf (COTS) based substrates have been in use for the design of metasurface [14], [15], [16], [17], [18]. These COTS based substrates are mostly made of Polytetrafluoroethylene (PTFE) materials [19], [20], [21] which are relatively expensive compared to other synthetic and natural composite materials, one of which is Glass Fiber Reinforced Polymer (GFRP) based composites [22]. A composite material [23] is an engineered product and is a combination of two or more materials, all having different properties.

GFRP based composites find several applications ranging from construction, marine, biomedical, electronics, automotive, and mechanical [24], [25], [26]. Different classes of families (S-glass, E-glass, D-glass, T-glass etc.) of Glass Fibers are used in combination with fillers and polymer matrices to form GFRP composites [26], [27]. These GFRP based composites exhibit better strength-to-weight ratio, electrical properties, high fracture toughness, and excellent corrosion and thermal resistance [23]. Based on GFRP properties, it is an ideal and suitable alternative option that can be used for metasurface antennas instead of PTFE based composites.

A. RESEARCH CONTRIBUTION

In this paper, the authors have firstly designed, simulated and developed a GFRP composite based metasurface patch antenna. We have compared the performance of the GFRP composite based metasurface patch antenna (simulated as well as measured results) against the performance of Linear C-band patch antenna and GFRP based metasurface patch antenna. The results obtained through simulation and testing show characteristic similarity thus validating the approach adopted for the printing of copper on GFRP composite. Using GFRP composite as a metasurface on top of simple microstrip patch antenna results in an overall 39% gain enhancement compared to simple microstrip patch antenna gain.

B. ORGANIZATION OF PAPER

Rest of the paper is organized as follows: Section 2 describes the design, simulation, fabrication, and measurement of the Linear C-band microstrip planar patch array antenna. Section 3 presents the design, simulation, fabrication, and measurement test results of GFRP composite (without any unit cells) on top of microstrip planar patch antenna with the basic aim for gain enhancement. Section 4 presents the design, simulation, fabrication, and measurement results of GFRP based Metasurface (with units cells) phased array antenna, along with its comparison with Section 2 and Section 3 results. Section 5 concludes the paper.

II. LINEAR C-BAND PATCH ANTENNA

In this section, the authors have presented the details of design and simulation as well as the fabrication process and measurement results of a linear C-band Patch antenna. A patch antenna is one of the most commonly used printed antennas and can be designed and analyzed either using transmission-line model [28] or cavity model [29]. The Transmission-line model is the easiest model compared to the cavity model, however, there are some inaccuracies associated with this method. Fringing effects take place in the microstrip patch antenna design due to finite dimensions length ‘L’ and width ‘W’. The design and simulation details are provided in the subsequent section.

A. DESIGN & SIMULATION C-BAND LINEAR MICROSTRIP PATCH ANTENNA

For designing of the C-band linear microstrip patch antenna, NELCO NY 9220 substrate was used with a dielectric permittivity (ε_r) of 2.2 and a thickness ‘t’ of 1.57 mm. The patch antenna needs to be designed at the center frequency ‘f_r’ of 5.5 GHz. In the transmission line model, dimensions of the patch antenna (W & L) and effective dielectric constant ‘ε_{eff}’ and effective length ‘L_{eff}’ is mathematically calculated using a sequence of a set of Equations from (Eq.1) to (Eq.5) [30].

$$W = \frac{1}{2f_r\sqrt{\mu_o\varepsilon_o}}\sqrt{\frac{2}{\varepsilon_r+1}} = \frac{\upsilon_o}{2f_r}\sqrt{\frac{2}{\varepsilon_r+1}} \tag{1}$$

$$\varepsilon_{reff} = \frac{\varepsilon_r+1}{2} + \frac{\varepsilon_r-1}{2}\left[1+12\frac{h}{W}\right]^{-\frac{1}{2}} \tag{2}$$

$$\frac{\Delta L}{h} = 0.412\frac{(\varepsilon_{reff}+0.3)(\frac{W}{h}+0.264)}{(\varepsilon_{reff}-0.258)(\frac{W}{h}+0.8)} \tag{3}$$

$$L = \frac{1}{2f_r\sqrt{\varepsilon_{reff}}\sqrt{\mu_o\varepsilon_o}} - 2\Delta L \tag{4}$$

$$L_{eff} = L + 2\Delta \tag{5}$$

Any inaccuracy associated with this transmission line model has been removed by optimizing the design in CST Studio Suite software [31]. We have used the equations derived by us and presented in [32] to calculate the dimensions of the patch antenna and then model the same in the CST Studio Suite software. Fig. 1, shows the isometric view of the microstrip patch antenna.

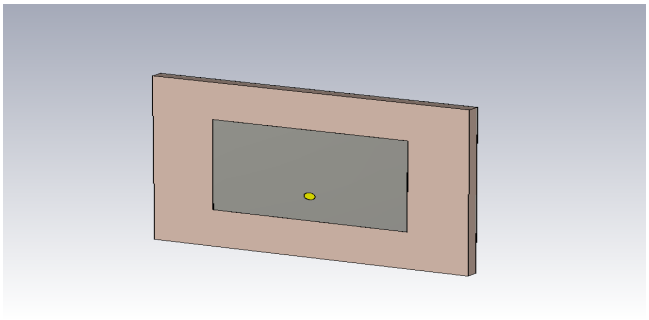

FIGURE 1. Isometric view of the design of Microstrip Patch Antenna in CST Studio Suite software.

Design has been simulated and optimized on the desired center frequency at 5.5 GHz and the modelled dimension of the patch antenna varies 1.0 mm in the length 'L' dimension and 0.2 mm in the width 'W' dimension compared to the calculated values using the above equations. Fig. 2, shows the simulated radiation pattern plot of co-polarization and cross-polarization of simple microstrip patch antenna and Fig. 3, shows the 3D radiation pattern of the microstrip patch antenna at 5.5 GHz with a maximum gain of 7.68 dBi.

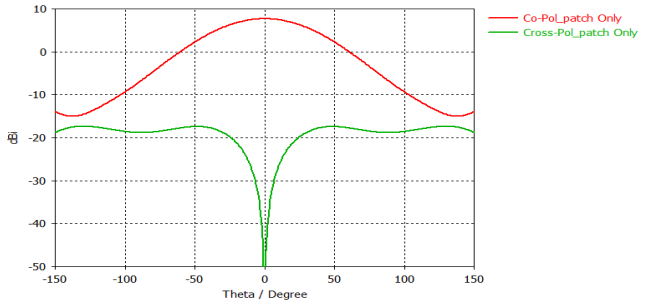

FIGURE 2. Simulated radiation pattern (Co-polarization and Cross polarization) of simple microstrip patch antenna at $\Phi = 0^{o}$.

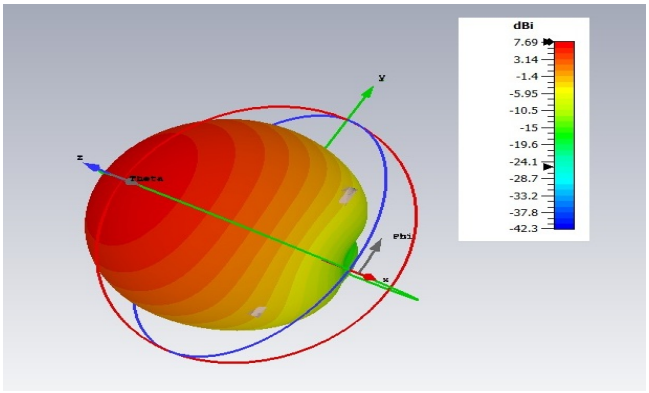

FIGURE 3. Simulated 3D radiation plot of C-band Microstrip Patch Antenna.

B. FABRICATION & MEASUREMENT C-BAND LINEAR MICROSTRIP PATCH ANTENNA

Once the design is optimized, probe-fed microstrip patch antenna is fabricated on the LPKF milling machine [33]. The need of low dielectric permittivity (ε_r) substrate is fulfilled by using NELCO NY9220 [36], which is a commercially available substrate, with a thickness 't' of 1.57 mm and dielectric permittivity (ε_r) of 2.2. Fig. 4, shows the fabricated microstrip patch antenna with dimensions highlighted. The fabricated antenna is tested on Rohde & Schwarz ® VNA for measurement of Input reflection coefficient (S_{11}). Fig. 5, depicts a matching trend between measurement and simulated data. Input impedance bandwidth of 220 MHz is achieved for VSWR < 2 (S_{11} < -10 dB).

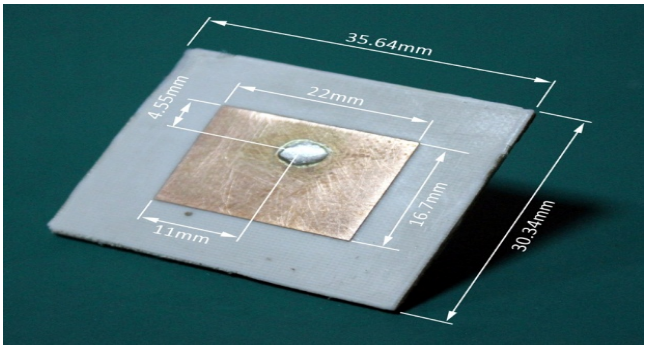

FIGURE 4. Fabricated microstrip patch antenna with dimensions.

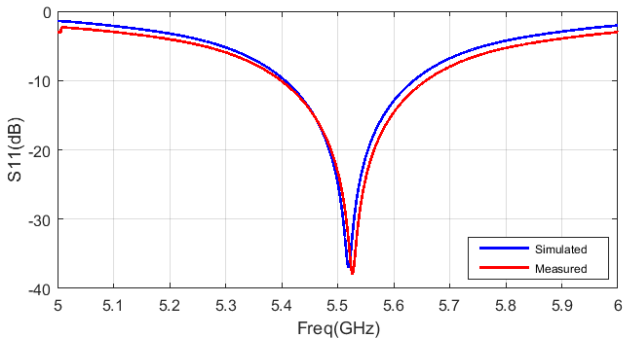

FIGURE 5. Measured and simulated plot of reflection coefficient of microstrip patch antenna.

The radiation pattern of fabricated microstrip patch antenna was measured in a specialized antenna testing facility, i.e. 'Anechoic Chamber'. Measurements were performed in the anechoic chamber while having a quiet zone area of 40 dB below and shielding effectiveness of 90 dB at the testing frequency range. Gain calculation and radiation pattern measurements are done using a wideband Standard Gain Horn (SGH) as a transmitting source and Antenna Under Test (AUT) which in this case is a microstrip patch antenna is mounted at the receiving end. Before taking any measurements, closed loop calibration is performed. After calibration, a microstrip patch antenna is mounted on a special type of platform in which measurements can be performed, both over roll axis and in the azimuth direction. Fig. 6, shows the view of microstrip patch antenna mounted on a fully automated platform in an anechoic chamber test facility, Two measurement cuts ($\Phi = 0^{o}$ and $\Phi = 90^{o}$) from θ

(- 150º to + 150º) with a step size of 1º and Intermediate Frequency Band Width (IFBW) of 100 Hz are taken in the azimuth plane. Different Φ values are obtained by rotating the roll axis by 90º. Measured data is then processed for the calculation of antenna gain value and its radiation pattern. The maximum gain of 7.5 dB is calculated at 5.5 GHz.

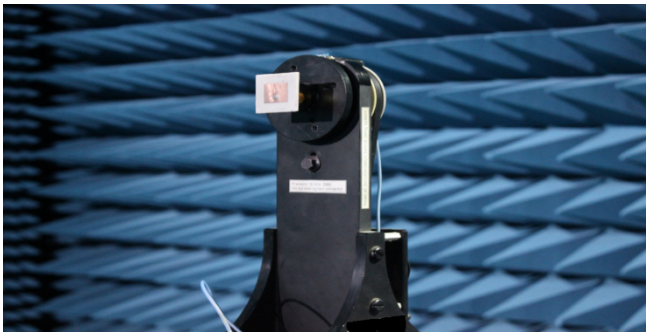

FIGURE 6. C-band Microstrip patch antenna mounted on an automated platform in Anechoic Chamber Test facility for the measurement of the Radiation pattern in E-plane & H-plane.

Fig. 7, shows the comparison of simulated and measured radiation pattern plots, both for E-plane (Φ = 0º) and H-plane (Φ = 90º). Fig. 7 (a and b), shows significant similarity between the measured and simulated data.

III. GFRP BASED METASURFACE PATCH ANTENNA

As discussed in the introduction section, GFRP finds promising applications and usage in antenna industry. In this section, the authors have presented the design, simulation, fabrication, and measurement detail of GFRP manufactured composite. The authors have designed, manufactured, and electrically characterized GFRP substrates in [32]. The thickness of the substrate has been selected 2.32 mm as it provides least dielectric permittivity (refer table 2 of [32]).
In this section, first simple GFRP composite sample is placed on top of a microstrip patch antenna with different gap values (λ/2, λ/4, λ/8) and the performance is analyzed for different gaps values. Then, GFRP based metasurface is introduced on top of the microstrip patch antenna and the performance in terms of any gain enhancement is analyzed.

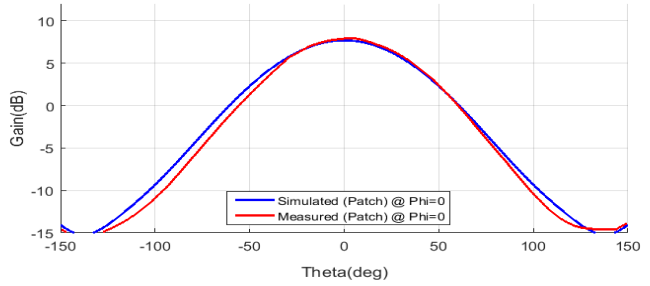

(a)

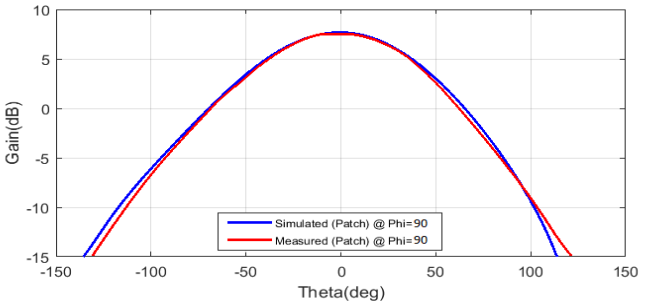

(b)

FIGURE 7. Comparison of Simulated and Measured Radiation Pattern of Patch Antenna at frequency 5.5 GHz (a) At Φ = 0º (b) At Φ = 90º.

A. DESIGN & SIMULATION OF GFRP BASED METASURFACE PATCH ANTENNA

Simple GFRP composite Sample-X is placed on top of the microstrip patch antenna as presented in Fig. 8. Simulation analysis are performed using three different scenarios for optimization having a gap between GFRP and microstrip patch antenna of λ/2, λ/4, λ/8. The optimal distance between the microstrip antenna and metasurface helps to minimize the reflections caused by the GFRP based metasurface. These effects becomes minimal, when the reflected wave from the surface of metasurface is in phase with the transmitted wave from microstrip patch antenna. (Eq.6), shows the optimal distance between the microstrip antenna and metasurface [32],

$$D = \frac{n * \lambda_o}{2} \tag{6}$$

Where 'D' is the distance between the microstrip antenna and metasurface. 'n' is 1,2,3…. and 'λ_o' is the free space wavelength. As can be seen in Fig. 9, placement of a simple GFRP sample at a distance of $\lambda_o/2$ (n = 1) from microstrip patch antenna gives a maximum gain value of 8.80 dBi, which shows an increase in gain value of 1.12 dB compared to simple microstrip patch antenna. For higher values of n > 2 distance is increased resulting in higher volume of metasurface antenna. Optimal distance of λ/2 is used in the further design of GFRP based metasurface patch antenna.

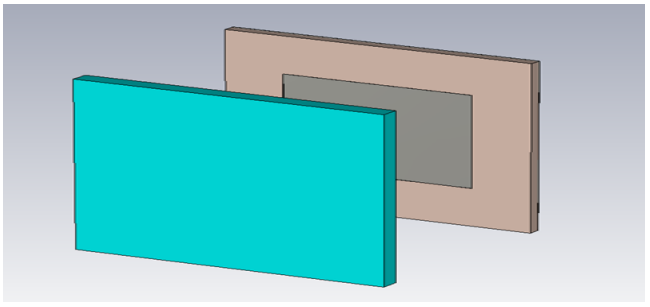

FIGURE 8. Isometric view of the simple GFRP composite sample placed in front of microstrip patch antenna.

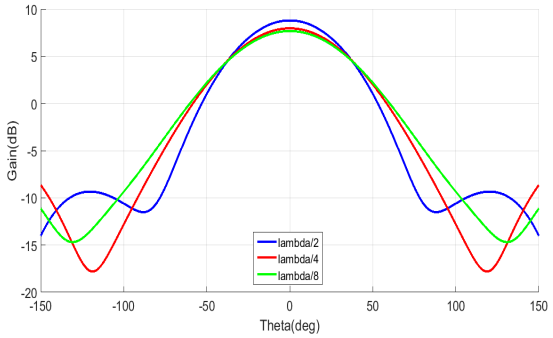

FIGURE 9. Simulated radiation pattern plot of simple GFRP composite sample placed on top of microstrip patch antenna at different gap values (λ/2, λ/4, λ/8).

Now, after optimizing the distance, design of GFRP based microstrip patch antenna can progress. Microstrip patch antenna design is the same that is discussed in Section 2 with NELCO NY9220 substrate used. Metasurface to be designed on top of microstrip patch antenna is a GFRP based composite sample with copper foil tape pasted (procedure discussed in [32]) on top of it. Rectangular shaped unit cells are designed on the GFRP composite and the design of unit cells is optimized in terms of length, width and spacing of unit cells. Fig. 10, shows the isometric view of metasurface antenna design with unit cells on the GFRP composite;

GFRP composite metasurface is placed at an optimized distance of λ/2 from the microstrip patch antenna. Fig. 11, shows the measured input reflection coefficient (S_{11}) value of the metasurface patch antenna. Resonant frequency is marginally close with design frequency of 5.5 GHz.

Fig. 12, shows the 3D radiation pattern plot of the metasurface patch antenna. Fig. 13 shows the simulated 2D rectangular plot of radiation pattern. The plots show Co-polarization and Cross-polarization results obtained by GFRP based composite metasurface patch antenna and the Linear C-band patch antenna at a distance of *λ/2*.

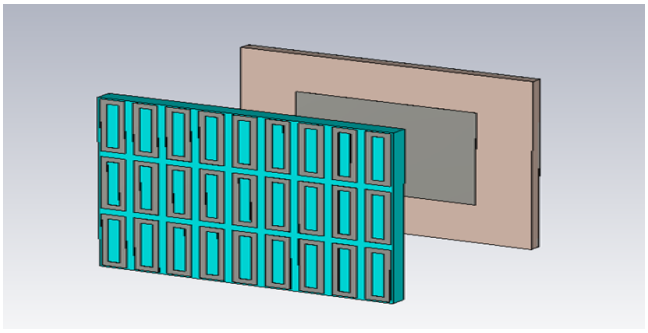

FIGURE 10. Simulated radiation pattern plot of simple GFRP composite sample placed on top of microstrip patch antenna at different gap values (λ/2, λ/4, λ/8).

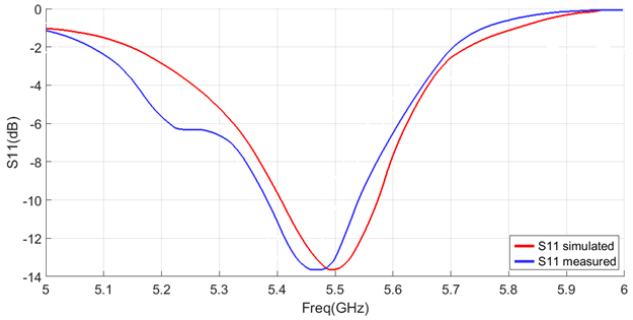

FIGURE 11. Input Reflection Coefficient (S_{11}) of GFRP based metasurface patch antenna.

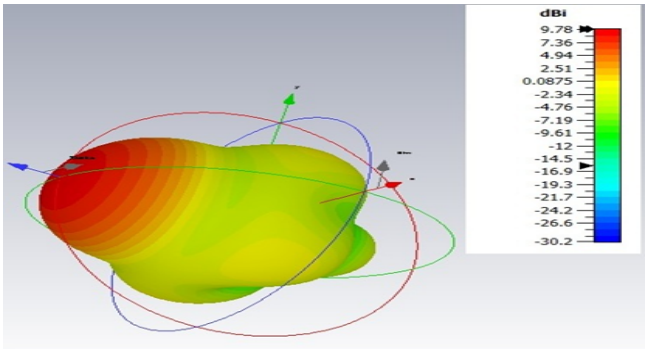

FIGURE 12. Simulated 3D radiation plot of GFRP based composite metasurface patch antenna.

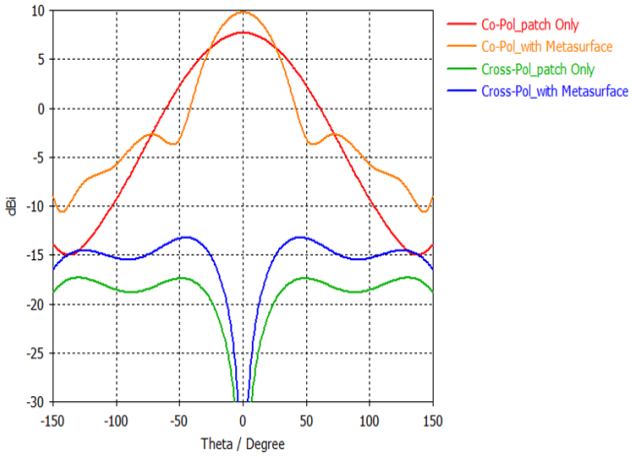

FIGURE 13. Simulated radiation pattern (Co-polarization and Cross-polarization) plot of GFRP based composite metasurface antenna at Φ = 0°.

B. FABRICATION & MEASUREMENT GFRP BASED METASURFACE PATCH ANTENNA

Fabrication of metasurface with unit cells is done through a chemical etching process. Fig.14, shows the fabricated metasurface along with the dimensions of the unit cell (Inner length = 7.7 mm, Inner Width = 1.4 mm). These dimensions have been obtained using parametric sweep (CST Studio Suite software) [31] in order to achieve gain enhancement. The metasurface is integrated with the microstrip patch antenna using Teflon screws. Fig. 15, shows the integrated

form of metasurface patch antenna.

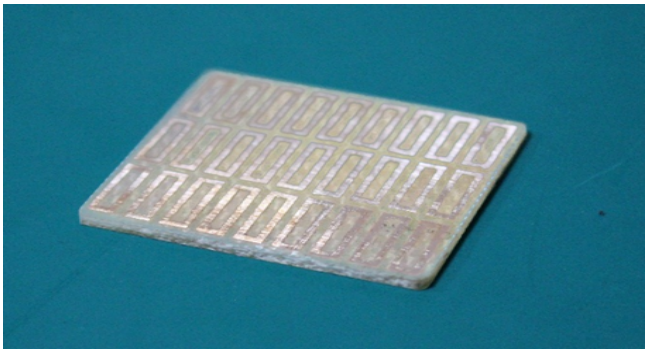

(a)

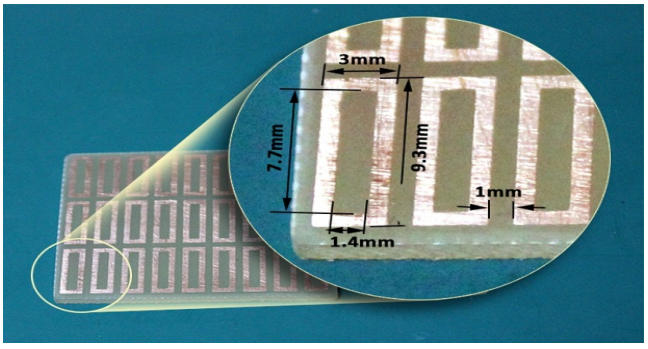

(b)

FIGURE 14. (a) Fabrication of unit cells on top of GFRP based composite used a metasurface (b) Zoom in view of the unit cells with dimensions.

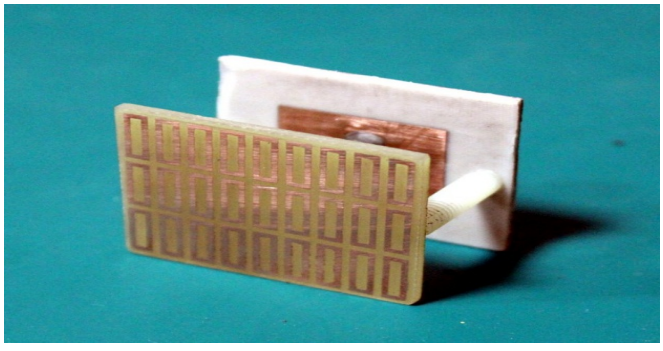

FIGURE 15. An integrated form of GFRP based metasurface with microstrip patch antenna.

For measurement purposes, simple GFRP with no unit cells is tested with a microstrip patch antenna in an anechoic chamber test facility. Next, the metasurface patch antenna is mounted on the platform in an anechoic chamber test facility and the measurements are repeated. Same measurement settings and the procedure is adopted for calculating the gain and measuring the radiation pattern of E-plane and H-plane. Fig. 16, shows the mounting view of a metasurface patch antenna on the automated platform.

FIGURE 16. GFRP metasurface patch antenna mounted on an automated platform at Anechoic Chamber test facility for radiation pattern measurement.

Fig.17, below shows the comparison of simulated and measured data of simple GFRP composite on top of microstrip patch antenna with a gap of λ/2. As can be seen, the measured plot agrees with the simulated data with a maximum gain of approximately 8.80 dBi. This results in an increased gain of 1.12 dB with the use of just a GFRP composite sample with no unit cells on top of it.

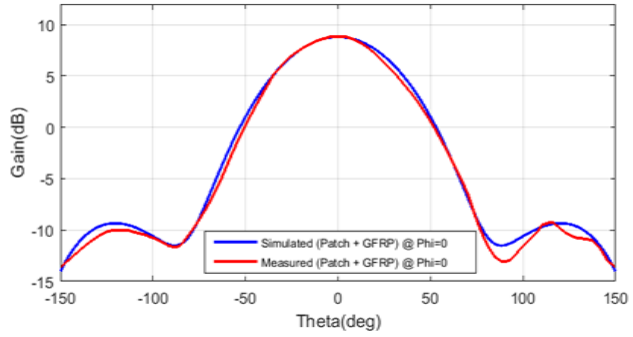

(a)

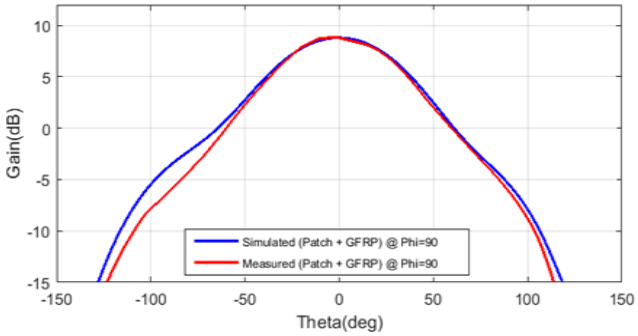

(b)

FIGURE 17. Comparison of Simulated and Measured Radiation Pattern of a simple GFRP with patch antenna at frequency 5.5 GHz (a) At Φ = 0° (b) At Φ = 90°.

Fig. 18, shows the comparison of simulated and measured data of GFRP based metasurface (with unit cells) on top of microstrip patch antenna with a gap of λ/2. As can be seen,

the measured plot is in agreement with the simulated data with a maximum gain of approximately 9.7 dBi. This results in an increased gain of 2.2 dB compared to simple microstrip patch antenna.

After analyzing the measurement results, it is found that there is a 15% enhancement of gain with the introduction of just a simple manufactured GFRP composite sample (X). Whereas, with the introduction of GFRP based composite metasurface, gain enhancement increased to 30% compared to simple microstrip patch antenna.

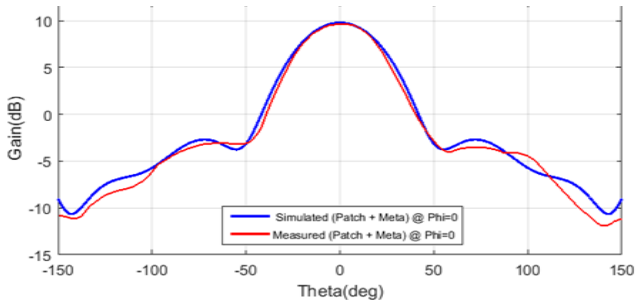

(a)

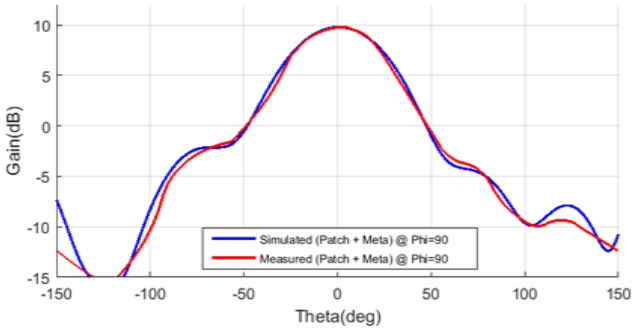

(b)

FIGURE 18. Comparison of Simulated and Measured Radiation Pattern of a GFRP based metasurface patch antenna at frequency 5.5 GHz (a) At $\Phi = 0°$ (b) At $\Phi = 90°$.

IV. GAIN ENHANCEMENT USING ADDITIONAL GFRP ON TOP OF METASURFACE PATCH ANTENNA

In this section, the metasurface patch antenna design discussed in the previous section is further explored for enhancement of overall gain. A simple manufactured GFRP composite sample is now placed in front of the GFRP based metasurface antenna and the performance is evaluated in terms of antenna gain enhancement.

A. DESIGN & SIMULATION

There are two different values of dielectric constant is used, i.e. NELCO NY 9220 the dielectric constant of is 2.2 and GFRP composite the dielectric constant is 4.5.

Fig. 19, shows the GFRP based composite sample having a thickness of 2.32 mm and permittivity of 4.5 is now placed in front of GFRP based metasurface patch antenna. Several iterations are performed to find the most suitable gap between the simple GFRP and GFRP based metasurface. At a gap of $\lambda/4$, simulated results show further promising results which are discussed in the next section.

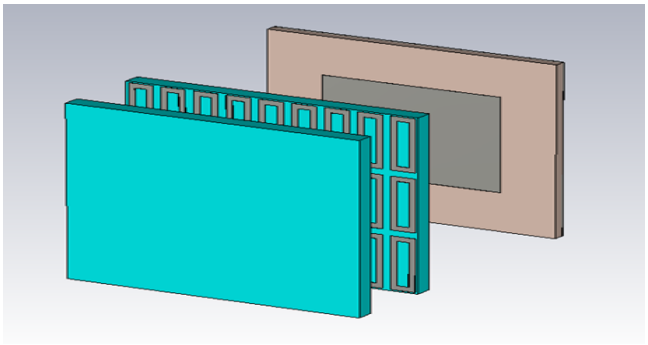

FIGURE 19. Isometric view of additional GFRP on top of GFRP based metasurface patch antenna.

B. FABRICATION & MEASUREMENT

Fabrication of a simple GFRP composite sample took place and Fig. 20, shows the microstrip patch antenna, GFRP based metasurface and simple GFRP composite sample. The antenna is integrated in such a manner that GFRP based metasurface is $\lambda/2$ on top of a microstrip patch antenna and a simple GFRP composite sample is $\lambda/4$ on top of GFRP based metasurface.

Integrated form of GFRP based metasurface antenna mounted on the automated platform is shown in Fig. 21. As can be seen in this Fig. 21, all layers are integrated through Teflon screws and measurement of radiation pattern and calculation of gain is done similarly as is done in earlier testing of antenna.

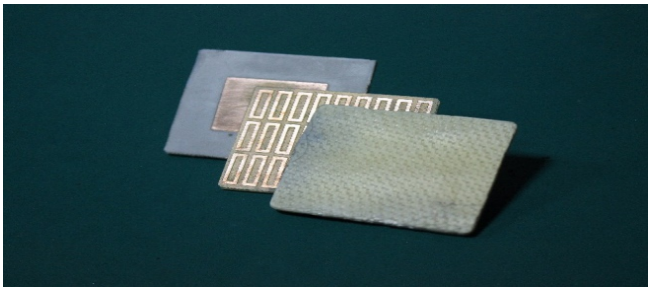

FIGURE 20. Manufactured C-band patch antenna with GFRP based metasurface and plain GFRP sample on top it.

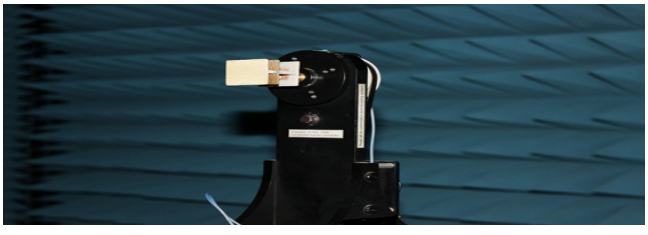

FIGURE 21. Integrated GFRP based metasurface antenna mounted on the platform at Anechoic Chamber Test facility for the measurement of the radiation pattern.

After carrying out the measurements, Figure 22 shows the comparison of simulated and measurement plots, both for E-plane (Φ = 0º) and H-plane (Φ = 90º). Measurement data shows significant conformance with simulated data with a maximum gain achieved is approximately 10.4 dBi with a further increase of gain of 0.7 dB compared to GFRP based metasurface. In this scenario, net increase of gain is 2.9 dB compared to the simple microstrip patch antenna which comes out to be 39% of gain increased overall.

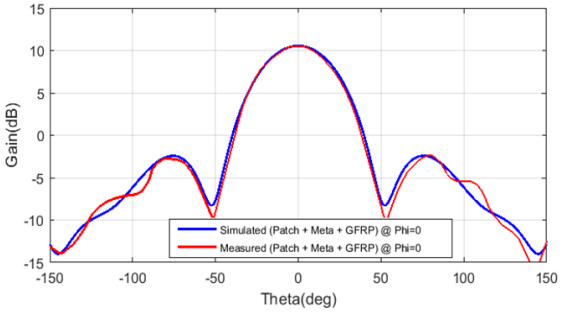

FIGURE 22. Comparison of Simulated and Measured Radiation Pattern of plain GFRP on top of GFRP based metasurface patch antenna at frequency 5.5 GHz at Φ = 0º.

V. CONCLUSION

In this paper, the feasibility of using an indigenously manufactured GFRP composite sample as a metasurface on top of a microstrip patch antenna is explored. In one of the previous work reported [35], the author achieved the enhancement of gain with the help of metasurface with the help of two parallel feeding slots using COTS based substrate. In this paper, the authors manage to achieve an increase of gain from 9 dBi to 12.4 dBi with a net increase of 37.77%. In the research activity discussed in this paper, initially C-band microstrip patch antenna was designed, optimized and tested with a net measurement gain of 7.5 dBi. Later, GFRP based composite metasurface is designed on top of the microstrip patch antenna and the measurement gain comes out to be 9.7 dBi with a net increase of 2.2 dB. Finally, another layer of plain GFRP sample is introduced on top of GFRP based metasurface patch antenna and the measurement gain comes out to be 10.4 dBi with a net overall gain increase of 2.9 dB. In the end, a 39% increase in gain is observed in comparison to simple microstrip patch antenna with the use of indigenously manufactured GFRP composite sample as metasurface. The net percentage increase in gain using GFRP composite is comparable or better than the one using COTS based substrate. These promising results of the GFRP composite sample provide a superior and better alternative solution as compared of using COTS based substrate (PTFE) for metasurface application.

REFERENCES

[1] M. Cao, L. Wang, H. Xu, D. Chen, C. Lou and N. Zhang, "Sec-D2D: A Secure and Lightweight D2D Communication System With Multiple Sensors," IEEE Access, vol. 7, pp. 33759-33770, 2019.

[2] A. Kiourti and J. L. Volakis, "Wearable antennas using electronic textiles for RF communications and medical monitoring," in 2016 10th European Conference on Antennas and Propagation (EuCAP), 2016.

[3] M. Herceg, G. Kaddoum, D. Vranješ and E. Soujeri, "Permutation Index DCSK Modulation Technique for Secure Multiuser High-Data-Rate Communication," IEEE Transactions on Vehicular Technology, vol. 67, pp. 2997-3011, 2018.

[4] D. Wentzloff, R. Blazquez, F. Lee, B. Ginsburg and J. Powell, "System design considerations for ultra-wideband communication," IEEE Communications Magazine, vol. 43, pp. 114-121, 2005.

[5] H. A. Majid, A. Rahim, M. Kamal, Hamid, M. Rijal and N. A. Murad, "Frequency-Reconfigurable Microstrip Patch-Slot Antenna," IEEE Antennas and Wireless Propagation Letters, vol. 12, pp. 218-220, 2013.

[6] T. Takahashi, Y. Konishi, S. Makino, S. Kabashima and T. Ozaki, "Super lightweight planar array antenna with stretched structure for satellite communication," in IEEE Antennas and Propagation Society International Symposium., 1999.

[7] E. Erdil, K. Topalli, M. Unlu, O. A. Civi and T. Akin, "Frequency Tunable Microstrip Patch Antenna Using RF MEMS Technology," IEEE Transactions on Antennas and Propagation, vol. 55, no. 4, pp. 1193-1196, 2007.

[8] S. Chattopadhyay, M. Biswas, J. Siddiqui and D. Guha, "Input impedance of probe-fed rectangular microstrip antennas with variable air gap and varying aspect ratio," IET Microwaves, Antennas & Propagation, vol. 3, no. 8, pp. 1151-1156, 2009.

[9] M. Martinis, K. Mahdjoubi, R. Sauleau, S. Collardey and Bernard, "Comparison of a cavity antenna with stacked patches and a metasurface-inspired design," in 9th European Conference on Antennas and Propagation (EuCAP), 2015.

[10] H.-T. Chen, A. J. Taylor and N. Yu, "A review of metasurfaces: physics and applications," Reports on progress in physics, vol. 79, no. 7, 2016.

[11] S. Sun, Q. He, J. Hao, S. Xiao and L. Zhou, "Electromagnetic metasurfaces: physics and applications," Advances in Optics and Photonics, vol. 11, no. 2, pp. 380-479, 2019.

[12] K. L. Chung and S. Chaimool, "Broadside gain and bandwidth enhancement of microstrip patch antenna using a MNZ-metasurface," Microwave and Optical Technology Letters, vol. 54, no. 2, pp. 529-532, 2011.

[13] X. Ding, S. Wu, Z. Zhao, Z. Nie and Qing-Huo Liu, "Meta-surface loading broadband and high-aperture efficiency dual circularly polarized patch antenna," International Journal of RF and Microwave Computer-Aided Engineering, vol. 31, no. 3, 2021.

[14] H. L. Zhu, X. H. Liu, S. W. Cheung and T. I. Yuk, "Frequency-Reconfigurable Antenna Using Metasurface," IEEE Transactions on Antennas and Propagation, vol. 62, no. 1, pp. 80-85, 2014.

[15] J. Hu, G. Q. Luo and Z.-C. Hao, "A Wideband Quad-Polarization Reconfigurable Metasurface Antenna," IEEE Access, vol. 6, pp. 6130-6137, 2018.

[16] H. Zhu, S. Cheung, Y. J. Guo, C. Ding and T. Yuk, "Aperture efficiency improvement using metasurface," in 10th European Conference on Antennas and Propagation (EuCAP), 2016.

[17] H. Zhu, K. L. Chung, X. L. Sun, S. W. Cheung and T. I. Yuk, "CP metasurfaced antennas excited by LP sources," in Proceedings of the 2012 IEEE International Symposium on Antennas and Propagation, 2012.

[18] M. Zhu and L. Sun, "Design of frequency reconfigurable antenna based on metasurface," in IEEE 2nd Advanced Information Technology, Electronic and Automation Control Conference, 2017.

[19] J. Aguilar, M. Beadle, P. Thompson and M. Shelley, "The microwave and RF characteristics of FR4 substrates," in IEE Colloquium on Low Cost Antenna Technology, 1998.

[20] P. S. Anjana, M. T. Sebastian, M. N. Suma and P. Mohanan, "Low dielectric loss PTFE/CeO2 ceramic composites for

microwave substrate applications," International Journal of Applied Ceramic Technology, vol. 5, no. 4, pp. 325-333, 2008.
[21] K. Murali, S. Rajesh, O. Prakash, A. Kulkarni and R. Ratheesh, "Comparison of alumina and magnesia filled PTFE composites for microwave substrate applications," Materials Chemistry and Physics, vol. 113, no. 1, pp. 290-295, 2009.
[22] B. Zimmerli, M. Strub, F. Jeger, O. Stadler and A. Lussi, "Composite materials: composition, properties and clinical applications. A literature review," Schweizer Monatsschrift fur Zahnmedizin= Revue mensuelle suisse d'odonto-stomatologie= Rivista mensile svizzera di odontologia e stomatologia, vol. 120, no. 11, pp. 972-986, 2010.
[23] T. Sathishkumar, S. Satheeshkumar and J. Naveen, "Glass fiber-reinforced polymer composites – a review.," Journal of Reinforced Plastics and Composites., vol. 33, no. 13, pp. 1258-1275, 2014.
[24] H. Quast, A. Keil and T. Loffler, "Investigation of foam and glass fiber structures used in aerospace applications by all-electronic 3D Terahertz imaging," in 35th international conference on infrared, millimeter, and terahertz waves, 2010.
[25] F. Heinrich and R. Lammering, "An experimental investigation on the adhesion of printed electronics on fiber reinforced composites," in 8th European Workshop on Structural Health Monitoring, EWSHM 2016, 2016.
[26] A. Gupta, H. Singh and R. Walia, "Effect of glass fiber and filler volume fraction variation on mechanical properties of GFRP composite," in Proceedings of the International Conference on Research and Innovations in Mechanical Engineering, 2014.
[27] A. Al Mahmood, A. Mobin, R. Morshed and T. Zaman, "Characterization of glass fibre reinforced polymer composite prepared by hand layup method," American journal of bioscience and bioengineering, vol. 5, no. 1, p. 8, 2017.
[28] H. Pues and A. Van de Capelle, "Accurate transmission-line model for the rectangular microstrip antenna," IET Proceedings on Micorwaves, Optics and Antennas, vol. 131, no. 6, pp. 334-340, 1984.
[29] A. Mohammad, H. Subhi, A. Ahmad and S. Juma, "Cavity model analysis of rectangular microstrip antenna operating in TM 03 mode," in 2nd International Conference on Information & Communication Technologies, 2006.
[30] C. A. Balanis, "Microstrip Antennas," in Antenna Theory Analysis & Design, John Wiley & Sons, 2005, pp. 817-820.
[31] CST Studio Suite, https://www.cati.com/software/cst-studio-suite/
[32] Ali, A. K. M. S. and I. Ahmed, "Electrical characterization of glass fiber reinforced polymer (GFRP) composites for future metasurface antenna applications." Materials Research Express 8(6): 1-9, 2021
[33] LPKFMilling Machine, https://www.lpkfusa.com/Products/pcb_prototyping/machines/
[34] C. Kumar, H. U. R. Mohammed and G. Peake, "mmWave Radar Radome Design Guide," Texas Instruments Incorporated, US, 2021.
[35] P. Hu and Y. Pan, "Wideband metasurface-based antenna with enhanced gain," in Asia-Pacific Microwave Conference (APMC), 2016.
[36] NELCO NY 9220 substrate Datasheet "https://rfshop.cz/nelco.pdf."